

HETEROCYCLES, Vol. 101, No. 1, 2020, pp. 273 - 283. © 2020 The Japan Institute of Heterocyclic Chemistry
Received, 11th June, 2019, Accepted, 16th July, 2019, Published online, 1st August, 2019
DOI: 10.3987/COM-19-S(F)23

CONFORMATIONAL PROPERTIES AND M₁ ANTIMUSCARINIC ACTIVITY OF 4-SUBSTITUTED PIRENZEPINE/TELENZEPINE ANALOGUES

Yuki Kanase,^a Kosho Makino,^b Takashi Yoshinaga,^c Hidetsugu Tabata,^a Tetsuta Oshitari,^a Hideaki Natsugari,^d and Hideyo Takahashi^{*b}

^aFaculty of Pharma Sciences, Teikyo University, 2-11-1 Kaga, Itabashi-ku, Tokyo 173-8605, Japan. ^bFaculty of Pharmaceutical Sciences, Tokyo University of Science, 2641 Yamazaki, Noda, Chiba 278-8510, Japan. ^cGlobal Cardiovascular Assessment, Eisai Co., Ltd., 5-1-3 Tokodai, Tsukuba, Ibaraki 300-2635, Japan. ^dFaculty of Pharmaceutical Sciences, The University of Tokyo, 7-3-1 Hongo, Bunkyo-ku, Tokyo 112-0033, Japan.

Abstract – The atropisomeric and conformational properties of the 4-Cl/Me-substituted pirenzepine/telenzepine analogues were examined. Although the 4-substitution is not effective in reducing the rotational barrier of the N5–(C1=O) bond, the butterfly motion of the tricyclic ring system was frozen. The atropisomers showed little racemization after heating at 80 °C for 5 days. While these analogues showed less affinity to the M₁ receptor compared with pirenzepine, a *ca.* 4.4-fold difference in potency between the atropisomers was observed for **1b**.

INTRODUCTION

Benzo-fused seven-membered-ring nitrogen-heterocycles serve as the scaffolds of many biologically active molecules.¹ We have investigated the conformations of such heterocycles and their relationships with their biological activities.² Since these heterocycles possess relatively flexible rings, the ring often changes its conformation so as to exert biological activity. In the course of our study on the relationship between physicochemical properties and biological activity, we became interested in freezing the butterfly motion of 5*H*-dibenz[*b,f*]azepine to provide the specific conformer.³ In terms of stereochemical properties, it should be noted that atropisomerism⁴ is latent in this tricyclic system. In the attempt to freeze the butterfly motion, the 4-substituted carbamazepine (5*H*-dibenz[*b,f*]azepine-5-carboxamide) was synthesized and the atropisomers were isolated with high stereochemical stability. Evaluation of the

inhibitory effects on hNav1.2 channel currents showed that the 4-Cl/Me-substituted carbamazepine derivatives showed greater inhibitory effects compared with carbamazepine. However, no difference in the activity between atropisomers was observed, implying that the atropisomerism in the 5*H*-dibenz[*b,f*]azepine structure of carbamazepine was not effective in exerting its biological activity.⁵ Therefore, we redirected our focus to the bioactive compounds related to 5*H*-dibenz[*b,f*]azepine, *i.e.*, pirenzepine and telenzepine. Pirenzepine is the first M₁-selective muscarinic receptor antagonist, which has been introduced into ulcer therapy.⁶ Telenzepine also exhibits a selectivity that is comparable to that shown by pirenzepine.⁷ Although a large number of conformational studies of pirenzepine and telenzepine have been performed, there have been few efforts to evaluate the biological activity of the atropisomers.⁸ In order to identify the physicochemical requirements for the potential M₁ selectivity, we therefore undertook the synthesis and biological evaluation of the 4-substituted pirenzepine and telenzepine analogues (**1a**, **b**) (Figure 1). We anticipated that the 4-substitution would sterically hinder the rotation of the N–C1' axis and the butterfly motion in the tricyclic ring system.

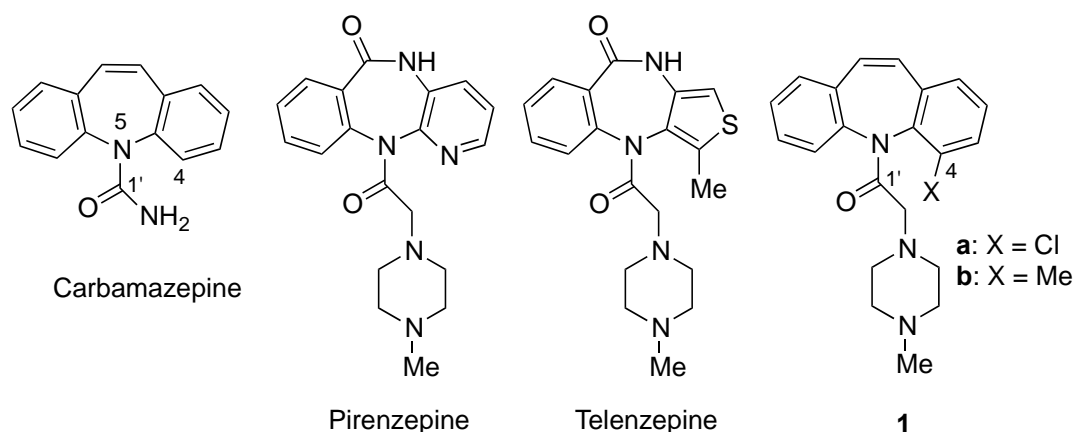
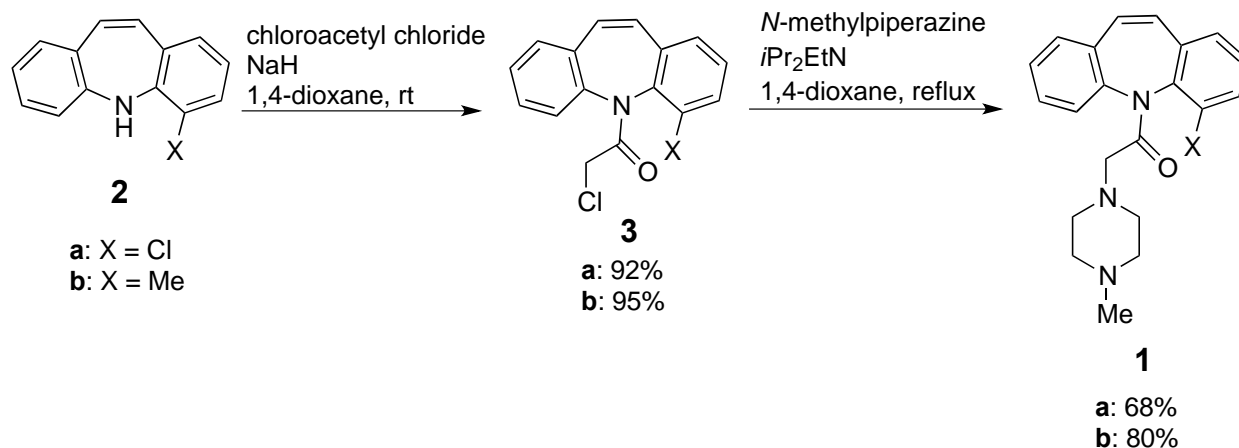


Figure 1. Carbamazepine, Pirenzepine, Telenzepine, and the analogues (**1a**, **b**)

RESULTS AND DISCUSSION

1. Preparation

4-Substituted pirenzepine/telenzepine analogues (**1a**, **b**) were prepared starting from 4-substituted iminostilbenes (**2a**, **b**),⁵ as shown in Scheme 1. The reaction of the iminostilbene **2** with chloroacetyl chloride in the presence of K₂CO₃ in 1,4-dioxane at room temperature afforded *N*-chloroacetyl intermediates (**3a**, **b**). Amination of **3** with *N*-methylpiperazine was performed in the presence of *i*Pr₂NEt in 1,4-dioxane under reflux conditions and afforded the analogues **1a**, **b** (Scheme 1).



Scheme 1. Preparation of 4-substituted analogues **1a, b**

2. Conformational study

The 4-substituted analogues **1a, b** theoretically have four stereoisomers, which are *E/Z*-amide isomers around the N–(C1'=O) bond (axis 5) and atropisomers based on the coordinated rotation of four *sp*²–*sp*² axes (axis 1–axis 4)⁹ (Figure 2).

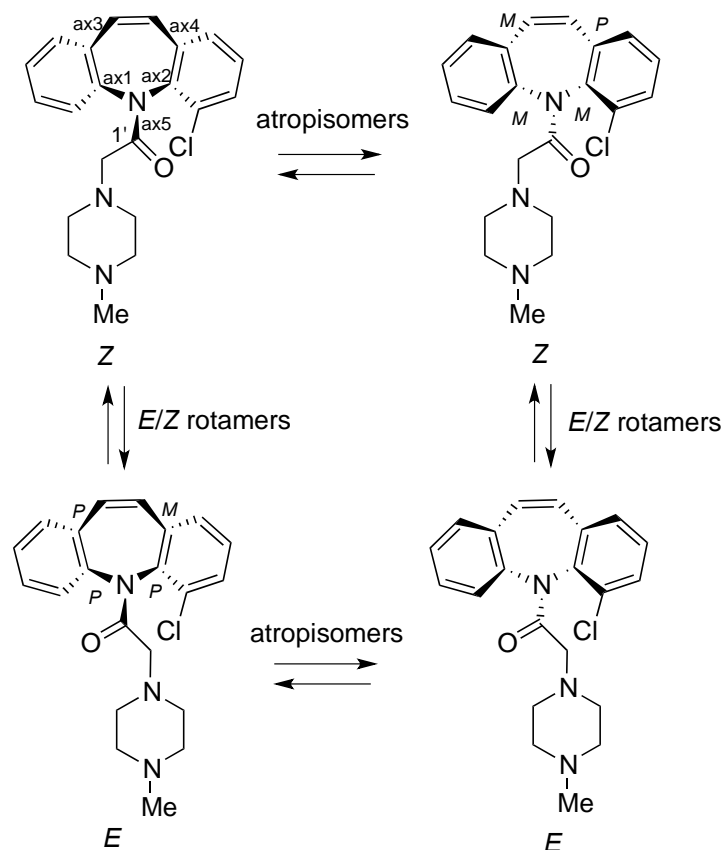


Figure 2. Four stereoisomers of **1a**

First, the conformation of compound **1a** was examined based on the ^1H NMR spectra in $\text{DMSO-}d_6$. At $23\text{ }^\circ\text{C}$, two sets of resonance corresponding to the *E/Z*-amide conformers were observed (*E/Z* = 1.7 : 1). Unfortunately, the *E/Z*-isomers could not be separated at room temperature using nonchiral HPLC, which implies that the rotational barrier of the $\text{N5}-(\text{C1}'=\text{O})$ bond (axis 5) is less than that required for the isolation of each conformer at room temperature. The activation free energy barrier (ΔG^\ddagger) to the rotation of axis 5 was estimated by VT-NMR based on the coalescence method¹⁰ (see the Supporting Information). It was revealed that the ΔG^\ddagger value should be 88 kJ/mol. Similarly, the conformation of compound **1b** was examined using ^1H NMR and VT-NMR. Two sets of resonance corresponding to the *E/Z*-amide conformers were observed (*E/Z* = 2.3 : 1) at $23\text{ }^\circ\text{C}$, and they could not be separated using nonchiral HPLC. The ΔG^\ddagger value of the rotation of axis 5 was estimated to be 80 kJ/mol (see the Supporting Information). Such low energy barriers of less than 100 kJ/mol indicated that the 4-substituted analogues **1a** and **1b** should exist as conformational mixtures at room temperature.

We further attempted to separate the atropisomers of **1a** and **1b**, and each atropisomer was successfully isolated using preparative chiral HPLC. The optical rotation of each atropisomer was then examined (Figure 3).

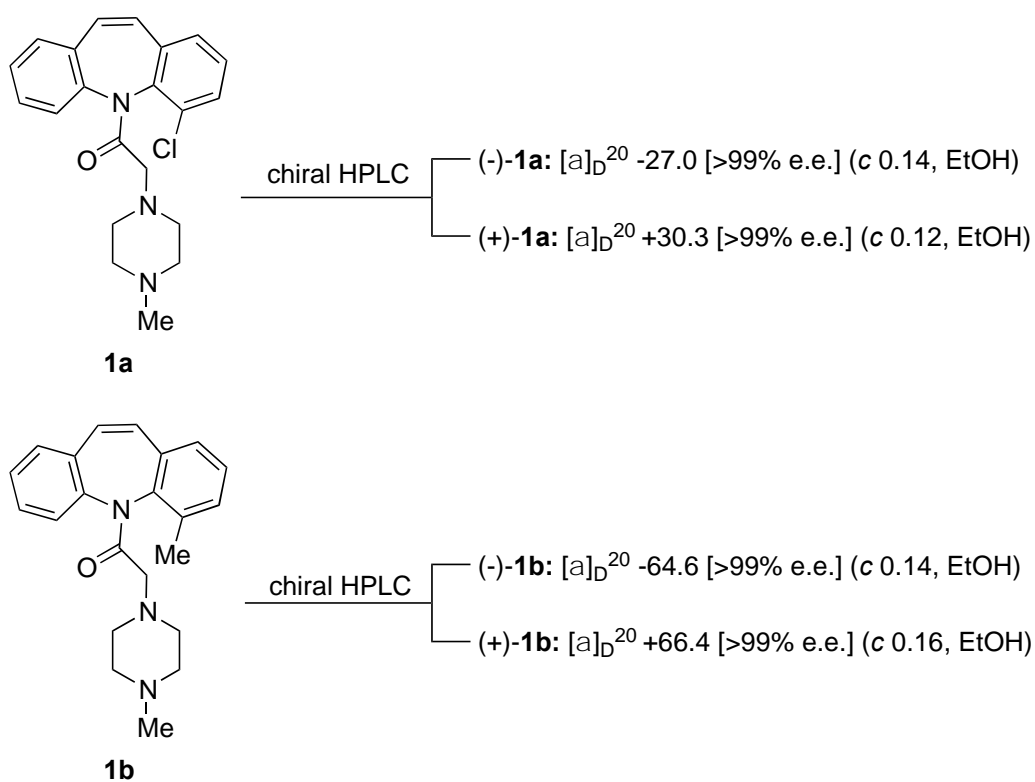


Figure 3. Separation of atropisomers of **1a** and **1b**

We examined the stereochemical stability of the atropisomers and found that it was surprisingly high: little racemization of each atropisomer of **1a** and **1b** was observed at 80 °C in toluene for 5 days, which means that the activation free energy barrier shown by the ΔG^\ddagger value should be more than 130 kJ/mol at the lowest (see the Supporting Information). Since the decomposition of the compounds at higher temperature was observed, we did not attempt to estimate their precise ΔG^\ddagger values.

For the determination of the absolute stereochemistry of the enantiomers of **1a** and **1b**, we fortunately succeeded in obtaining the atropisomers (+)-**1a** and (-)-**1b** as single crystals. The X-ray structural analysis¹¹ revealed that the structure of (+)-**1a** is (*M,M,M,P*)¹² and that of (-)-**1a** is (*P,P,P,M*). Similarly, the X-ray structural analysis revealed that the structure of (-)-**1b** is (*M,P,M,P*) and that of (+)-**1b** is (*P,M,P,M*)¹³ (Figure 4).

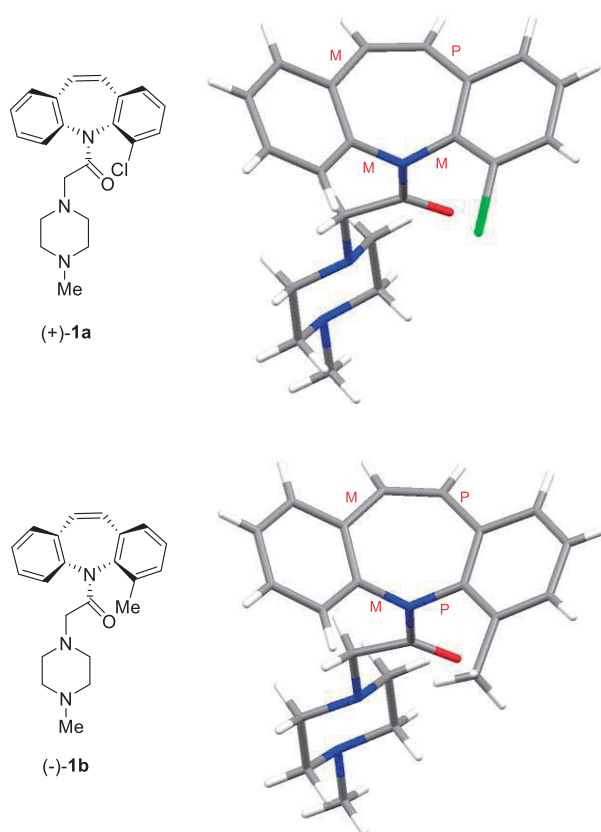


Figure 4. X-Ray crystal structures of the optically active compounds (+)-**1a** and (-)-**1b**

3. Biological results

Finally, we evaluated the binding affinity to the M₁ receptor of analogues **1a** and **1b** in Ca²⁺ mobilization assays (see the Supporting Information). **1a** and **1b** in the racemic forms showed less potent affinity compared with pirenzepine. Considering that these analogues lack the amide (lactam) moiety in the central seven-membered ring, the existence of the amide group in the tricyclic ring system should be

important. In terms of atropisomerism, the atropisomers and the racemate in **1a** exhibited similar levels of affinity. In contrast, **1b** showed a *ca.* 4.4-fold difference in potency between the enantiomers [active eutomer: (–)-**1b** and less active distomer: (+)-**1b**] with median potency in the racemate (Table 1). It should be noted that the absolute stereochemistry in (–)-**1b** is a clue to the physicochemical requirements for the potential M₁ selectivity.

Table 1. In vitro affinity for the M₁ receptor

Compound	[α] _D rotation	IC ₅₀ (nM)
1a	(+/-)	294.9
	(–)	269.9
	(+)	262.4
1b	(+/-)	124.9
	(–)	51.4
	(+)	382.8
Pirenzepine		15.2

CONCLUSION

The atropisomeric and conformational properties of the 4-substituted pirenzepine analogues were examined to reveal that the substitution at the 4-position of the tricyclic ring system is effective for freezing the butterfly motion. Although the *E/Z*-amide conformers were not isolated, the atropisomers were isolated with surprisingly high stability. Compared with pirenzepine, these analogues showed lower binding affinity to the M₁ receptor. However, **1b** showed a *ca.* 4.4-fold difference in potency between the enantiomers. These findings may be useful for the future design of new M₁ receptor-selective drugs.

EXPERIMENTAL

General remarks: All reagents were purchased from commercial suppliers and used as received. Reaction mixtures were stirred magnetically, and the reactions were monitored by thin-layer chromatography (TLC) with precoated silica gel plates. Column chromatography was performed using silica gel (45–60 μ m). Extracted solutions were dried over anhydrous MgSO₄ or Na₂SO₄. Solvents were evaporated under reduced pressure. NMR spectra were recorded on a spectrometer at 600 MHz for ¹H NMR, and 150 MHz for ¹³C NMR at 296 K unless otherwise stated. Chemical shifts are given in parts per million (ppm) downfield from tetramethylsilane as an internal standard, and coupling constants (*J*) are

reported in Hertz (Hz). Splitting patterns are abbreviated as follows: singlet (s), doublet (d), triplet (t), quartet (q), multiplet (m), and broad (br). The high-resolution mass spectra (HRMS) were obtained with an ionization mode of ESI. IR spectra were recorded on an FT-IR spectrometer equipped with ATR (Diamond). Optical rotations were determined with a digital polarimeter. Melting points were recorded on a melting point apparatus and are uncorrected.

4-Chloro-5-chloroacetyl-5H-dibenz[*b,f*]azepine (3a). To a solution of 4-chloro-5H-dibenz[*b,f*]azepine **2a** (288 mg, 1.0 mmol) in 1,4-dioxane (10 mL) under argon were added successively NaH (60% in oil; 120 mg, 3.0 mmol) and chloroacetyl chloride (0.20 mL, 2.5 mmol), and the mixture was stirred at 23 °C for 25 h, then water (10 mL) was added and extracted with AcOEt. The organic layer was washed with brine and dried over Na₂SO₄. After concentration *in vacuo*, the residue was purified by silica gel column chromatography (AcOEt–hexane, 1 : 4) to give **3a** (281 mg, 0.923 mmol, 92%): ¹H NMR (600 MHz, CDCl₃) (*E:Z* = 1.3:1) (*E*-isomer) δ 7.67 (1H, d, *J* = 7.2 Hz), 7.55-7.48 (2H, m), 7.44 (2H, m), 7.31-7.27 (2H, m), 7.01-6.97(2H, m), 3.97 (1H, d, *J* = 13.8 Hz), 3.74 (1H, d, *J* = 13.8 Hz). (*Z*-isomer) δ 7.61 (1H, d, *J* = 7.2 Hz), 7.55-7.48 (2H, m), 7.42 (1H, dd, *J* = 7.8, 1.8 Hz), 7.38 (1H, m), 7.33 (2H, m), 7.05 (1H, d, *J* = 12 Hz), 6.95 (1H, d, *J* = 12 Hz), 4.04 (1H, d, *J* = 13.8 Hz), 3.75 (1H, d, *J* = 13.8 Hz). ¹³C NMR (150 MHz, CDCl₃) (*E*-isomer) δ 165.4, 138.4, 137.7, 135.8, 134.9, 133.1, 131.0, 130.1, 130.0, 129.9, 129.7, 129.0, 128.7, 127.9, 127.8, 41.1. (*Z*-isomer) δ 166.4, 139.3, 135.9, 134.8, 133.4, 132.5, 132.5, 129.9, 129.8, 129.5, 129.3, 128.8, 128.6, 128.3, 128.1, 41.6. IR (ATR) 1697 cm⁻¹; HRMS (ESI) *m/z* calcd for C₁₆H₁₁NOCl₂Na 326.0110 (M+Na)⁺, found 326.0111.

5-Chloroacetyl-4-methyl-5H-dibenz[*b,f*]azepine (3b). To a solution of 4-methyl-5H-dibenz[*b,f*]azepine **2b** (76.6 mg, 0.37 mmol) in 1,4-dioxane (3.7 mL) under argon were added successively NaH (60% in oil; 44.4 mg, 1.11 mmol) and chloroacetyl chloride (58.7 μL, 0.74 mmol), and the mixture was stirred at 23 °C for 15 h, then water (10 mL) was added and extracted with AcOEt. The organic layer was washed with brine and dried over Na₂SO₄. After concentration *in vacuo*, the residue was purified by silica gel column chromatography (AcOEt–hexane, 1 : 4) to give **3b** (100 mg, 0.352 mmol, 95%): ¹H NMR (600 MHz, CDCl₃) (*E:Z* = 2:1) (*E*-isomer) δ 7.56 (1H, d, *J* = 8.4 Hz), 7.49-7.40 (3H, m), 7.38-7.36 (2H, m), 7.31-7.22 (1H, m), 7.01 (1H, d, *J* = 11.4 Hz), 6.91 (1H, d, *J* = 11.4 Hz), 3.89 (1H, d, *J* = 12.6 Hz), 3.68 (1H, d, *J* = 12.6 Hz), 2.50 (3H, s). (*Z*-isomer) δ 7.52 (1H, d, *J* = 7.8 Hz), 7.49-7.40 (3H, m), 7.38-7.36 (1H, m), 7.31-7.22 (2H, m), 6.98 (1H, d, *J* = 11.4 Hz), 6.95 (1H, d, *J* = 11.4 Hz), 3.82 (1H, d, *J* = 13.8 Hz), 3.63 (1H, d, *J* = 13.8 Hz) 2.56 (3H, s), ¹³C NMR (150 MHz, CDCl₃) (*E*-isomer) δ 165.7, 138.8, 138.4, 136.3, 135.3, 133.7, 132.3, 131.2, 129.6, 129.5, 128.8, 128.6, 127.8, 127.5, 127.2, 41.3, 18.1. (*Z*-isomer) δ 166.8, 139.9, 136.9, 135.8, 135.5, 133.9, 131.3, 131.2, 129.7, 129.5, 129.4, 128.5, 128.1, 128.0, 127.3, 41.4, 18.1, IR (ATR) 1693 cm⁻¹; HRMS;(ESI) *m/z* calcd for C₁₇H₁₄NOCINa 306.0656 (M+Na)⁺, found 306.0656.

(4-Chloro-5H-dibenz[*b,f*]azepin-5-yl)-2-(4-methyl-1-piperazinyl)ethanone (1a). To a solution of 4-chloro-5-chloroacetyl-5H-dibenz[*b,f*]azepine **3a** (290.3 mg, 0.95 mmol) in 1,4-dioxane (9.5 mL) under argon were added successively *N,N*-diisopropylethylamine (*ca.* 10% in *N,N*-dimethylformamide; 0.82 mL, 4.77 mmol) and 1-methylpiperazine (0.33 mL, 4.77 mmol), and the mixture was stirred at reflux for 24 h, cooled down, and water (10 mL) was added and extracted with AcOEt. The organic layer was washed with 1N HCl aq., 1N NaOH aq., and brine and dried over Na₂SO₄. After concentration *in vacuo*, the residue was purified by silica gel column chromatography (MeOH(MeOH:NH₃ aq. = 10: 1)–CH₂Cl₂, 1: 8) to give **1a** as colorless crystals (237 mg, 0.643 mmol, 68%): mp 145–147 °C: ¹H NMR (600 MHz, CDCl₃) (*E:Z* = 1.1:1) (*E*-isomer) δ 7.65 (1H, d, *J* = 7.8 Hz), 7.51–7.48 (2H, m), 7.42–7.37 (2H, m), 7.35–7.33 (1H, m), 7.31–7.22 (1H, m), 6.95 (2H, s), 3.08 (1H, d, *J* = 15 Hz), 2.77 (1H, d, *J* = 15 Hz), 2.35 (8H, br), 2.24 (3H, s). (*Z*-isomer) δ 7.65 (1H, d, *J* = 7.8 Hz), 7.59 (1H, d, *J* = 7.8 Hz), 7.47–7.43 (2H, m), 7.42–7.37 (1H, m), 7.31–7.22 (2H, m), 7.00 (1H, d, *J* = 11.4 Hz), 6.92 (1H, d, *J* = 11.4 Hz), 3.06 (1H, d, *J* = 15 Hz), 2.86 (1H, d, *J* = 15 Hz), 2.35 (8H, br), 2.22 (3H, s). ¹³C NMR (150 MHz, CDCl₃) (*E*-isomer) δ 169.5, 139.2, 136.1, 134.9, 133.6, 133.4, 130.3, 129.6, 129.6, 129.4, 129.4, 128.8, 128.4, 128.3, 127.7, 59.5, 55.0, 55.0, 53.3, 53.2, 46.2. (*Z*-isomer) δ 168.5, 139.8, 137.7, 136.5, 135.8, 132.6, 132.3, 130.8, 129.6, 129.3, 129.2, 128.6, 128.3, 127.9, 127.7, 59.4, 55.0, 55.0, 53.3, 53.2, 46.2. IR (ATR) 1681 cm⁻¹; HRMS (ESI) *m/z* calcd for C₂₁H₂₃N₃OCl 368.1524 (M+H)⁺, found 368.1525.

(4-Methyl-5H-dibenz[*b,f*]azepin-5-yl)-2-(4-methyl-1-piperazinyl)ethanone (1b). To a solution of 5-chloroacetyl-4-methyl-5H-dibenz[*b,f*]azepine **3b** (295 mg, 1.04 mmol) in 1,4-dioxane (10 mL) under argon were added successively *N,N*-diisopropylethylamine (*ca.* 10% in *N,N*-dimethylformamide; 0.89 mL, 5.19 mmol) and 1-methylpiperazine (0.36 mL, 5.19 mmol), and the mixture was stirred at reflux for 26 h, cooled down, and water (10 mL) was added and extracted with AcOEt. The organic layer was washed with 1N HCl aq., 1N NaOH aq., and brine and dried over Na₂SO₄. After concentration *in vacuo*, the residue was purified by silica gel column chromatography (MeOH(MeOH:NH₃ aq. = 10: 1)- CH₂Cl₂, 1: 8) to give **1b** as colorless crystals (289 mg, 0.831 mmol, 80%): mp 133–135 °C: ¹H NMR (600 MHz, CDCl₃) (*E:Z* = 2:1) (*E*-isomer) δ 7.48–7.47 (1H, m), 7.42–7.37 (2H, m), 7.32–7.30 (1H, m), 7.27–7.20 (3H, m), 6.97 (1H, d, *J* = 11.4 Hz), 6.89 (1H, d, *J* = 11.4 Hz), 3.07 (1H, d, *J* = 15.6 Hz), 2.66 (1H, d, *J* = 15.6 Hz), 2.47 (3H, s), 2.43 (8H, br), 2.26 (3H, s). (*Z*-isomer) δ 7.48–7.47 (1H, m), 7.46–7.43 (1H, m), 7.42–7.37 (2H, m), 7.35–7.33 (1H, m), 7.32–7.30 (1H, m), 7.27–7.20 (1H, m), 6.94 (1H, d, *J* = 11.4 Hz), 6.91 (1H, d, *J* = 11.4 Hz), 2.88 (1H, d, *J* = 16.2 Hz), 2.67 (1H, d, *J* = 16.2 Hz), 2.53 (3H, s), 2.43 (8H, br), 2.25 (3H, s). ¹³C NMR (150 MHz, CDCl₃) (*E*-isomer) δ 168.7, 139.5, 138.9, 136.5, 135.3, 134.0, 131.0, 130.9, 129.4, 129.0, 128.8, 128.2, 127.8, 127.5, 127.1, 59.5, 54.9, 54.9, 53.0, 45.9, 29.8, 18.2. (*Z*-isomer) δ 169.9, 140.3, 137.5, 135.7, 135.5, 134.1, 132.1, 132.1, 129.7, 129.5, 129.2, 128.5, 128.0, 127.7, 127.1, 58.9, 54.9, 54.9, 53.1, 45.9, 29.8, 18.2.

Separation of the compounds into the stereoisomers, and those of physicochemical properties.

1a: CHIRALPAK IE (0.25 cm ϕ \times 25 cm); eluent, hexane/EtOH/0.1% DEA (3:2); flow rate, 0.4 mL/min; temperature, 23 °C; detection, 254nm; Former peak: retention time = 29.3 min; $[\alpha]_D^{20}$ +30.3 [$>99\%$ e.e.] (*c* 0.12, EtOH). Latter peak: retention time = 32.4 min; $[\alpha]_D^{20}$ -27.0 [$>99\%$ e.e.] (*c* 0.14, EtOH).

1b: CHIRALPAK AD-H (0.25 cm ϕ \times 25 cm); eluent, hexane/2-propanol/0.1% DEA (7:3); flow rate, 0.4 mL/min; temperature, 23 °C; detection, 254nm; Former peak: retention time = 13.9 min; $[\alpha]_D^{20}$ +66.4 [$>99\%$ e.e.] (*c* 0.16, EtOH). Latter peak: retention time = 16.0 min; $[\alpha]_D^{20}$ -64.6 [$>99\%$ e.e.] (*c* 0.14, EtOH).

Crystal data of (+)-1a and (-)-1b: All measurements were made on a Rigaku Raxis Rapid imaging plate area detector with graphite monochromated Cu-K α radiation. The data were collected at a temperature of -100 °C. The structure was solved by direct method SIR92 and expanded using Fourier techniques. The non-hydrogen atoms were refined anisotropically. All calculations were performed using the Crystal Structure (Crystal Structure 4.0) crystallographic software package or SHELXL97.

Crystal data of (+)-1a (CCDC: 1917491). C₂₁H₂₂ON₃Cl: mp 145-147 °C, *M_r* = 367.88, CuK α (λ = 1.54187 Å), orthorhombic, *P*2₁2₁2₁, colorless, block 0.150 \times 0.150 \times 0.100 mm, crystal dimensions *a* = 10.0840(4) Å, *b* = 11.1326(4) Å, *c* = 16.8528(5) Å, α = 90°, β = 90°, γ = 90°, *T* = 173 K, *Z* = 2, *V* = 1891.92(11) Å³, *D*_{calc} = 1.291 gcm⁻³, μ CuK α = 18.960 cm⁻¹, *F*₀₀₀ = 776.00, GOF = 1.421, *R*_{int} = 0.0517, *R*₁ = 0.0978, *wR*₂ = 0.2460.

Crystal data of (-)-1b (CCDC: 1917492). C₂₂H₂₅ON₃: mp 133-135 °C, *M_r* = 347.46, CuK α (λ = 1.54187 Å), orthorhombic, *P*2₁2₁2₁, colorless, block 0.200 \times 0.150 \times 0.100 mm, crystal dimensions *a* = 10.1399(3) Å, *b* = 11.2338(4) Å, *c* = 16.7850(6) Å, α = 90°, β = 90°, γ = 90°, *T* = 173 K, *Z* = 4, *V* = 911.96(11) Å³, *D*_{calc} = 1.207 gcm⁻³, μ CuK α = 5.899 cm⁻¹, *F*₀₀₀ = 744.00, GOF = 1.620, *R*_{int} = 0.0780, *R*₁ = 0.1083, *wR*₂ = 0.2282.

Biological evaluation using Ca²⁺ assay

Functional assays for human M₁ receptors were conducted using hM₁ receptor expressing BHK (baby hamster kidney) cell lines. After 30min later incubation with compounds at room temperature, carbachol (Sigma-Ardorich Co. LLC.) was added as an agonist. Intracellular Ca²⁺ intensity was measured by FDSS7000 (Hamamatsu Photonics K.K.) and IC₅₀ values of each compounds were calculated.

ACKNOWLEDGEMENTS

This work was supported in part by Grants-in-Aid for Scientific Research (C) (19K06980) from the Japan Society for the Promotion of Science.

REFERENCES AND NOTES

1. For recent review articles on medium-ring benzo-fused nitrogenous heterocycles, see: (a) J. H. Ryan, C. Hyland, A. G. Meyer, J. A. Smith, and J. X. Yin, *Prog. Heterocycl. Chem.*, 2012, **24**, 493; (b) K. Ramig, *Tetrahedron*, 2013, **69**, 10783.
2. (a) S. Lee, T. Kamide, H. Tabata, H. Takahashi, M. Shiro, and H. Natsugari, *Bioorg. Med. Chem.*, 2008, **16**, 9519; (b) H. Tabata, K. Akiba, S. Lee, H. Takahashi, and H. Natsugari, *Org. Lett.*, 2008, **10**, 4871; (c) H. Tabata, H. Suzuki, K. Akiba, H. Takahashi, and H. Natsugari, *J. Org. Chem.*, 2010, **75**, 5984; (d) H. Tabata, J. Nakagomi, D. Morizono, T. Oshitari, H. Takahashi, and H. Natsugari, *Angew. Chem. Int. Ed.*, 2011, **50**, 3075; (e) H. Tabata, N. Wada, Y. Takada, T. Oshitari, H. Takahashi, and H. Natsugari, *J. Org. Chem.*, 2011, **76**, 5123; (f) H. Tabata, N. Wada, Y. Takada, J. Nakagomi, T. Miike, H. Shirahase, T. Oshitari, H. Takahashi, and H. Natsugari, *Chem. Eur. J.*, 2012, **18**, 1572; (g) H. Tabata, T. Yoneda, T. Oshitari, H. Takahashi, and H. Natsugari, *J. Org. Chem.*, 2013, **78**, 6264; (h) T. Yoneda, H. Tabata, J. Nakagomi, T. Tasaka, T. Oshitari, H. Takahashi, and H. Natsugari, *J. Org. Chem.*, 2014, **79**, 5717; (i) T. Yoneda, H. Tabata, T. Tasaka, T. Oshitari, H. Takahashi, and H. Natsugari, *J. Med. Chem.*, 2015, **58**, 3268; (j) H. Tabata, T. Yoneda, S. Ito, T. Tasaka, T. Oshitari, H. Takahashi, and H. Natsugari, *J. Org. Chem.*, 2016, **81**, 3136; (k) H. Tabata, T. Yoneda, T. Oshitari, H. Takahashi, and H. Natsugari, *J. Med. Chem.*, 2017, **60**, 4503; (l) H. Tabata, K. Murai, K. Funaki, C. Takemae, T. Tasaka, T. Oshitari, H. Takahashi, and H. Natsugari, *Heterocycles*, 2017, **99**, 566.
3. Y. Kanase, M. Kuniyoshi, H. Tabata, Y. Takahashi, S. Kayama, S. Wakamatsu, T. Oshitari, H. Natsugari, and H. Takahashi, *Synthesis*, 2015, **47**, 3907.
4. For recent review articles on axial chirality and atropisomerism, see: (a) J. Clayden, W. J. Moran, P. J. Edwards, and S. R. LaPlante, *Angew. Chem. Int. Ed.*, 2009, **48**, 6398; (b) S. R. LaPlante, P. J. Edwards, L. D. Fader, A. Jakalian, and O. Hucke, *ChemMedChem*, 2011, **6**, 505; (c) S. R. LaPlante, L. D. Fader, K. R. Fandrick, D. R. Fandrick, O. Hucke, R. Kemper, S. P. F. Miller, and P. J. Edwards, *J. Med. Chem.*, 2011, **54**, 7005; (d) A. Zask, J. Murphy, and G. A. Ellestad, *Chirality*, 2013, **25**, 265; (e) K. Ramig, *Tetrahedron*, 2013, **69**, 10783; (f) E. Kumarasamy, R. Raghunathan, M. P. Sibi, and J. Sivaguru, *Chem. Rev.*, 2015, **115**, 11239.
5. Y. Kanase, T. Kitada, H. Tabata, K. Makino, T. Oshitari, H. Ohashi, T. Yoshinaga, H. Natsugari, and H. Takahashi, *Bioorg. Med. Chem.*, 2018, **26**, 2508.
6. (a) R. Hammer and A. Giachetti, *Life Sci.*, 1982, **31**, 991; (b) B. H. Jaup, R. W. Stockbrugger, and G. Doteval, *Scand. J. Gastroenterol. Suppl.*, 1982, **17**, 119.
7. (a) M. Eltze, S. Gönne, R. Riedel, B. Shlotke, C. Schudt, and W. A. Simon, *Eur. J. Pharmacol.*, 1985, **112**, 211; (b) M. Eltze, *Eur. J. Pharmacol.*, 1988, **151**, 205.
8. (a) W. G. Eberlein, G. Trummelitz, W. W. Engel, G. Schmidt, H. Pelzer, and N. Mayer, *J. Med. Chem.*,

- 1987, **30**, 1378; (b) W. G. Eberlein, W. W. Engel, G. Trummlitz, G. Schmidt, and R. Hammer, *J. Med. Chem.*, 1988, **31**, 1169; (c) Y. Karton, B. J. Bradbury, J. Baumgold, R. Paek, and K. A. Jacobson, *J. Med. Chem.*, 1991, **34**, 2133; (d) J. Feeney and C. Pascual, *J. Pharm. Pharmacol.*, 1984, **36**, 187; (e) G. Trummlitz, G. Schmidt, H.-U. Wagner, and P. Luger, *Arzneim.-Forsch.*, 1984, **34**, 849; for an article on the existence of enantiomers of telenzepine, see: (f) P. Eveleigh, E. C. Hulme, C. Schudt, and N. J. M. Birdsall, *Mol. Pharmacol.*, 1989, **35**, 477.
9. In this paper, we denote the absolute stereochemistry of compound **1** as *M/P* (chiral helical nomenclature). The terms *M* and *P* correspond to *aS* and *aR* based on the chiral axis.
 10. A. Lewis, T. J. Rutherford, J. Wilkie, T. Jenn, and D. Gani, *J. Chem. Soc., Perkin Trans. 1*, 1998, 3795.
 11. The absolute stereochemistry was determined based on the Flack parameter.
 12. The terms *P* and *M* (chiral axis nomenclature) are listed in the order corresponding to axis 1 to axis 4 shown in Figure 2.
 13. CCDC 1917491 [(+)-**1a**], CCDC 1917492 [(-)-**1b**] contain the supplementary crystallographic data for this paper. These data can be obtained free of charge from The Cambridge Crystallographic Data Centre via www.ccdc.cam.ac.uk/data_request/cif.